

Interplay of atomic and solid-state effects in inner-shell-resonant photoelectron spectra

M. Elango*

*Institute of Experimental Physics and Technology, Tartu University, Ülikooli 18, EE2400 Tartu, Estonia
and Institute of Physics, Estonian Academy of Sciences, Riia 142, EE2400 Tartu, Estonia*

R. Ruus, A. Kikas, A. Saar, and A. Ausmees†

Institute of Physics, Estonian Academy of Sciences, Riia 142, EE2400 Tartu, Estonia

I. Martinson

Department of Atomic Spectroscopy, Lund University, Sölvegatan 14, S-223 62 Lund, Sweden

(Received 22 September 1995)

We report photoelectron spectra of metal chlorides excited in the vicinity of the chlorine $2p$ absorption edge. The spectra of RbCl, which has a narrow valence band, exhibit a strong resonance behavior. Hartree-Fock calculations show that the absorption final states are the atomiclike Frenkel excitons. Their decay is dominated by the Auger process where the final-state $4s$ and $3d$ electrons behave as spectators. In the sequence of chlorides with increasing width of the valence band the atomiclike resonance effects are continuously replaced by the bandlike shape of the spectra.

An interesting experimental procedure, combining inner-shell resonant-photoelectron and Auger spectroscopy, and made available by the recent development of combined synchrotron radiation and electron spectroscopy techniques, has already exposed its ability to disclose complex dynamics of inner-shell excitations of atoms,¹ molecules,² and different types of solids.³⁻⁵ For nonmetallic solids, the phenomena connected with this procedure have been especially clearly emphasized in the $2p$ -resonant photoelectron spectra of elements for which the $3p$ shell is the outermost filled shell. The elements at the end of the second period, such as silicon⁶ and phosphorus,⁷ which form semiconductors with wide $3p$ -related valence bands, expose very weak (if any) resonance effects, the main feature being the appearance of the $L_{23}M_{23}M_{23}$ normal Auger spectrum at the ionization threshold of the $2p$ shell. Contrary, the argonlike ions of potassium, calcium, and scandium in ionic solids exhibit strong resonance effects,^{3,8} characteristic for the Auger-resonant inelastic scattering.¹

Here we report the results of a study for the L_{23} absorption edge of Cl^- ions, constituents of metal chlorides. This choice puts us into an intermediate situation between the two groups of atoms (ions) described above, and gives hope to build a link between them.

The experiments are performed using synchrotron radiation from beamline 22 at the MAX-laboratory, Lund University, Sweden. The monochromator is a modified SX-700 plane grating monochromator with energy resolution of 0.13 eV in the actual photon energy region. The electron spectra are recorded by a hemispherical analyzer Scienta SES-200 with energy resolution of 0.075 eV. The samples, the films of metal halides, are evaporated *in situ* from a molybdenum boat onto a stainless-steel substrate. The film thickness (about 100 Å) is controlled by a quartz monitor. Other experimental details are described in Ref. 3.

In Fig. 1 a set of electron spectra of RbCl induced by photons in the region of the Cl^- L_{23} absorption edge is

shown. The absorption spectrum measured in the electron yield mode is exposed in the inset. Considering the absorption final states as the empty s - and d -like conduction-band states the comparison with the band-structure calculations⁹ leads to the scenario where the first few absorption maxima reflect the core excitons at the Γ_1 and X_3 points of the Brillouin zone (see, e.g., Ref. 10).

Three groups of lines may be distinguished in the electron spectra (Fig. 1). All spectra, starting from the bottom spectrum, the nonresonant pre-edge spectrum, show the Cl^- $3p$ valence band, the Rb^+ $4p$, Cl^- $3s$, and Rb^+ $4s$ photoelectron lines. With increasing photon energy this group keeps a constant binding energy. The intensity of the photoelectron lines does not exhibit any noticeable changes in the resonance regions, indicating a minor role of the participator Auger transitions in the decay of corresponding excitations. The second group is made up of the $L_{23}M_{23}M_{23}$ normal Auger lines composed of two sets of the 1S , 1D , and 3P terms of the final $3p^{-2}$ electron configuration shifted relative to each other by the 1.6-eV spin-orbit splitting of the $2p$ shell. This group has a constant kinetic energy. When the photon energy approaches the first absorption maximum, the third group of bands appears between the first and second groups. This group clearly exhibits a resonance behavior: it is fully developed at the maximum of the first absorption band (spectrum 5), almost disappears in the region between the first and second absorption bands, and reappears with a modified shape in the regions of the second (spectrum 9) and third (spectrum 13) absorption maxima.

For these spectra we use the theoretical model applied to analogous spectra of K^+ in Ref. 3. We treat an inner-shell excitation and its Auger decay as a two-step process. For the first step, the absorption process, the energies, and intensities of the $2p^6-2p^54s(3d)$ transitions in the Cl^- ion are calculated in the intermediate coupling scheme and the Hartree-Fock-Pauli approximation in conjunction with the Watson sphere model. The depth of the potential well at the Cl^- site

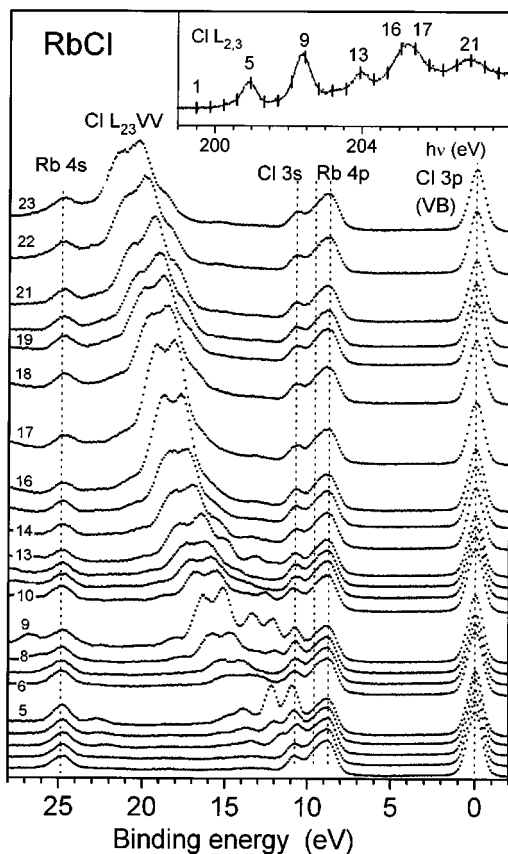


FIG. 1. Photoemission spectra for RbCl. The $\text{Cl}^- L_{2,3}$ absorption edge is shown in the inset. The number at each spectrum corresponds to the vertical bar with the same number in the inset and shows the photon energy used. The spectra are normalized to equal photon flux. The energy levels and corresponding Auger transitions are indicated for most of the structures. The binding energy is related to the valence-band maximum.

V_c is taken equal to 7.65 eV, the Madelung energy of the RbCl crystal, which leads to the mean radii of 5.8 (9.8) a.u. for the $4s(3d)$ orbitals. The calculated energies of the transitions $2p_{3/2}-4s$, $2p_{1/2}-4s$, $2p_{3/2}-3d$, and $2p_{1/2}-3d$ in Cl^- ions are 200.0, 201.6, 202.3, and 203.9 eV, respectively. They are reasonably close to the energies of the first three absorption maxima (200.9, 202.4, and 204.0 eV, respectively). Moreover, the calculated intensity ratio of these transitions, 33:50:17 (the second transition is here considered as a superposition of the transitions $2p_{1/2}-4s$ and $2p_{3/2}-3d$) is also very close to the observed intensity ratio 28:60:12 of these maxima. This comparison indicates that the interpretation of the absorption spectrum in terms of atomlike Frenkel excitons may well compete with the traditional interpretation based on the calculated structure of the undisturbed conduction band.¹⁰

For the second step, the Auger process, the normal $2p^5-3p^4$ as well as the spectator $2p^5 4s(3d)-3p^4 4s(3d)$ transitions are calculated. The radial integrals (F^k, G^k) for Auger final states are reduced by comparison with their Hartree-Fock values [by 30 and 25% for the $3p^4$ and $3p^4 4s(3d)$ configurations, respectively]. As this calculation overestimates the decay rates to the 3P term of the final configuration, the term intensities in the normal and $4s$ -spectator Auger spectra of Cl^- are corrected by scaling fac-

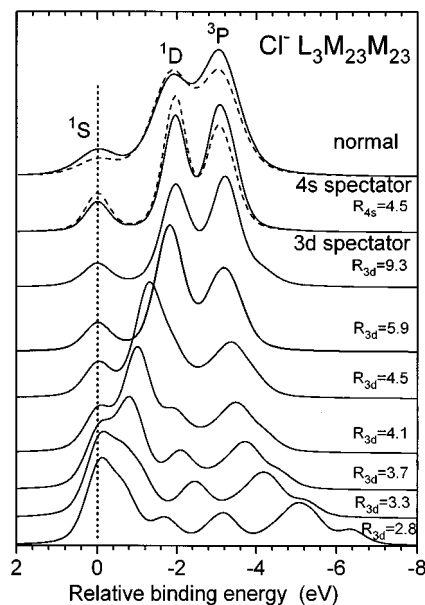


FIG. 2. Calculated $\text{Cl}^- L_3 M_{23} M_{23}$ Auger spectra for RbCl. The zero binding energy corresponds to the transition energy of the highest level of the final ionic configuration. The normal, $4s$, and $3d$ spectator spectra are broadened by the Voigt function with FWHM of 1.1, 0.7, and 0.8 eV, respectively. The depth of the Watson sphere for the $3d$ -spectator Auger spectra varies from zero (the uppermost spectrum) to 16.3 eV (the bottom spectrum). The mean radius of the spectator electron R_{3d} in the final ionic configuration is indicated at each spectrum. The dashed spectra are corrected ones using the experimental data for argon atoms (see text).

tors which lead to the correct description of analogous experimental spectra of the isoelectronic Ar atoms.¹¹ Some of the calculated Auger spectra are shown in Fig. 2.

Spectrum 5 of Fig. 1, after subtraction of the background and photoelectron lines represented by the pre-edge spectrum 1, is reproduced in Fig. 3(a). The calculated $4s$ -spectator $L_3 M_{23} M_{23}$ Auger spectrum well fits most of it. The remaining part (the broken curve) in the high-binding-energy region well fits the calculated normal $L_3 M_{23} M_{23}$ Auger spectrum. This similarity shows that the intensity of the participator process ($2p^{-1} 4s-3s^{-1}$) is negligible (this process should result in the resonant enhancement of the single-peak photoelectron line). In addition, the absence of the resonant enhancement of the valence ($\text{Cl}^- 3p$) band shows that the overlap of the wave functions of the loosely bounded excited electron and the core electron (which is included in the radial integral for participator process, but not included in the case of spectator process) is small, which is natural for the $4s$ excited state. So, the resonant structure may be unambiguously assigned to the $2p^5 4s-3p^4 4s$ pure-spectator Auger transition, shifted by 2.5 eV to the higher energy relative to the normal Auger spectrum.

Spectrum 9 of Fig. 1 is reproduced in Fig. 3(b). It may be understood as a superposition of three properly weighted components: (i) the $4s$ -spectator $L_2 M_{23} M_{23}$ Auger transition which originates from the decay of the $2p_{1/2} 4s$ state, (ii) the normal $L_3 M_{23} M_{23}$ Auger transition, which reflects ionization of the $2p_{3/2}$ subshell, and (iii) the $3d$ -spectator $L_3 M_{23} M_{23}$ Auger transition, which arises from the $2p_{3/2} 3d$ state. The calculated $2p_{3/2} 3d-3p^4 3d$ Auger spectrum is very sensitive

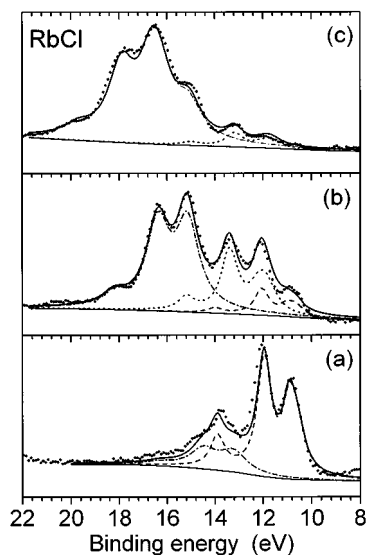


FIG. 3. The resonant photoemission spectra 5 (a), 9 (b), and 13 (c) from Fig. 1 (filled circles) and their components. The nonresonant background and photoelectron lines (spectrum 1 in Fig. 1) are subtracted. The Voigt functions which represent the calculated normal (dash-dotted line, FWHM=1.2 eV), 4s-spectator (dashed line, FWHM=0.7 eV), and 3d-spectator (dotted line, FWHM=0.8 eV) contributions to measured spectra and the resulting theoretical spectrum (solid line) are shown. The calculated spectra are shifted in the energy scale to fit the experimental spectra (by about 2–3 eV).

to the choice of V_c and, thus, to the mean radius of the 3d wave function of the final configuration R_{3d} . The small values of R_{3d} , which correspond to the collapsed 3d electron, lead to a spectrum very similar to the corresponding spectra of Ar (Ref. 11) and K^+ (Ref. 3). With increasing R_{3d} the spectrum obtains the two-band structure observable for Cl^- . If we change the fit parameter V_c systematically, the best fit for the third component of the spectrum is obtained with $V_c=4.35$ eV ($R_{3d}=5.9$ a.u.). Thus, the main effect of the spectator 3d electron is the 3.0-eV high-energy shift of the normal Auger spectrum together with some modification of its shape. Note that although in these general terms the effects of the 4s and 3d spectators on the $L_{23}M_{23}M_{23}$ Auger spectra are very similar, the careful comparison allows us to distinguish them firmly and use them as fingerprints of excitations of different nature. The underlying physics reduces mainly to the different multiplet coupling in the $3p^{-2}4s$ and $3p^{-2}3d$ configurations.

In Fig. 3(c) the Auger spectrum excited at the third absorption maximum (spectrum 13 of Fig. 1) is shown. It is dominated by the normal $L_{23}M_{23}M_{23}$ structure. In its low-energy part the resonant 3d-spectator $L_2M_{32}M_{23}$ structure is clearly visible and proves the *d* character of states responsible for this absorption band.

The normal Auger spectrum may be firmly identified in all spectra starting from spectrum 6 (Fig. 1). This means that above a photon energy of about 201.3 eV the transition electron has a noticeable probability of leaving the reaction region before or during the Auger transition. In a solid, such a threshold is naturally interpretable as the bottom of the conduction band for transitions from the $2p_{3/2}$ shell. However, the spurs of the normal $L_3M_{23}M_{23}$ structure may also be

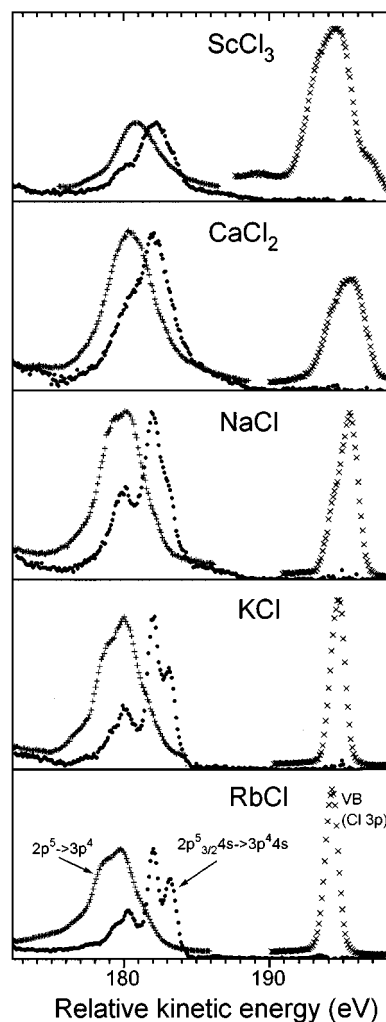


FIG. 4. The resonant (filled circles) and normal (crosses) Auger spectra and valence-band photoelectron spectra (sloping crosses) for several chlorides. The photoelectron lines are subtracted from the resonant spectra. The spectra are excited correspondingly at the first L_{23} absorption structures, far from the ionization thresholds (the photon energies used are 206 eV for $ScCl_3$, 220 eV for NaCl, KCl, and $CaCl_2$, and 212 eV for RbCl), and below absorption edges of corresponding compounds. The spectra are aligned to match the maxima of the resonant spectra. The Auger spectra of each compound are normalized to equal height.

found in the spectra excited with lower-energy photons indicating that the ionization threshold is rather smooth. This may be due to some inhomogeneous broadening of the threshold and/or to shake-up of the near-threshold excited electrons. The shape of a particular normal Auger spectrum depends on the relative weight of its L_3 and L_2 components. So, the spectra 12–14 and 18–23 clearly exhibit the 3P band of the $L_2M_{23}M_{23}$ spectrum, indicating that the absorption bands at 204.0 and 206.8 eV reflect transitions from the L_2 shell. Instead, the absorption band at 205.2 eV may be related to transitions from the L_3 shell.

Thus, the creation and decay of excitations related to the chlorine 2p shell of RbCl may be reasonably well understood in terms of atomic processes within chlorine ions. The main qualitative solid-state effect is the existence of an ionization threshold above which the transition electron is trans-

ferred into the conduction band. To disclose how much this atomiclike behavior is related to the extremely narrow valence band (VB) of RbCl we have studied the evolution of the resonant and normal $L_{23}M_{23}M_{23}$ Auger spectra in a sequence of chlorides with different VB widths. In Fig. 4 these spectra for RbCl, KCl, NaCl, CaCl_2 , and ScCl_3 are compared. The full width at half maximum (FWHM) of the VB of these compounds was estimated as 1.0, 1.1, 1.7, 2.8, and 3.0 eV, respectively, for RbCl, KCl, and NaCl in good accordance with the recent data of Ref. 12. The main effect, clearly seen in Fig. 4, is that with increasing VB width the resonant as well as normal Auger structures become wider and approach each other. The resonant spectrum loses its atomiclike nature characteristic for narrow-VB RbCl and obtains the solid-state nature characteristic for wide-VB semiconductors.^{6,7}

To conclude, we have shown, that the photoelectron and Auger spectra of RbCl exhibit a strong resonance behavior when the energy of incident photons passes through the L_{23} absorption edge of chlorine. Somewhat surprisingly, the spectra may be understood in terms of atomic transitions. In the sequence of chlorides with increasing VB width the atomiclike resonance effects are continuously replaced by the bandlike shape of the spectra. These results clarify the regularities of the structure of the $2p$ -resonant electron spectra of other solids.

The investigations were financially supported by the Estonian Science Foundation, the Swedish Natural Science Research Council, the Swedish Institute, and the International Science Foundation. The authors wish to thank Dr. E. Nõmiste, Dr. R. Nyholm, and Dr. A. Maiste for their assistance and discussions.

*Deceased.

[†]Present address: Department of Physics, University of Uppsala, Box 530, S-75121 Uppsala, Sweden.

¹G. B. Armen *et al.*, Phys. Rev. Lett. **54**, 1142 (1985).

²W. Eberhardt, in *Applications of Synchrotron Radiation*, edited by W. Eberhardt (Springer, Berlin, 1995), p. 203.

³M. Elango *et al.*, Phys. Rev. B **47**, 11 736 (1993).

⁴H. Wang *et al.*, Phys. Rev. A **50**, 1359 (1994).

⁵W. Drube, R. Treusch, and G. Materlik, Phys. Rev. Lett. **74**, 42 (1995).

⁶K. L. I. Kobayashi, H. Daimon, and Y. Murata, Phys. Rev. Lett.

50, 1701 (1983); R. A. Riedel *et al.*, *ibid.* **52**, 1568 (1984).

⁷T. Kendelewicz *et al.*, Phys. Rev. B **30**, 2263 (1984); T. Takashi *et al.*, *ibid.* **33**, 1485 (1986).

⁸A. Saar *et al.*, Phys. Rev. B **51**, 3202 (1995).

⁹Y. Onodera and Y. Toyozawa, J. Phys. Soc. Jpn. **22**, 833 (1967).

¹⁰M. Watanabe, J. Phys. Soc. Jpn. **34**, 755 (1973).

¹¹M. Meyer, E. von Raven, and B. Sonntag, Phys. Rev. A **49**, 3685 (1994); L. O. Werme, F. Bergmark, and K. Siegbahn, Phys. Scr. **8**, 149 (1973).

¹²G. K. Wertheim *et al.*, Phys. Rev. B **51**, 13 675 (1995).